

Rotational dynamics of axially symmetric solutes in isotropic liquids. I. A collective cage description from molecular dynamics simulations

Antonino Polimeno^{a)}

Baker Laboratory of Chemistry, Cornell University, Ithaca, New York 14853-1301

Giorgio J. Moro

Department of Physical Chemistry, University of Padova, Via Loredan 2, 35131 Padova, Italy

Jack H. Freed

Baker Laboratory of Chemistry, Cornell University, Ithaca, New York 14853-1301

(Received 21 December 1994; accepted 15 February 1995)

An operational definition of collective cage variables previously introduced for liquid argon is extended, via a molecular dynamics study, to the rotational properties of axially symmetric molecules. Quantitative measures of the static and dynamic cage properties are extracted for liquid Cl₂ near the triple point. The collective cage variables are well described by the potential acting on an arbitrary molecule (i.e. solute) for a fixed configuration of the other molecules (i.e. solvent). A dynamic separability of the solute orientation relative to the cage potential and of the relative solute displacement is justified in part by the faster relaxation found for the latter. Large and persistent orientational cage potentials ($\sim 15\text{--}20 k_B T$) lead to substantial alignment of the solute in the cage with an average local order parameter of 0.87. The reorientational correlation times for the *cage* are consistent with axially symmetric Brownian motion. The reorientational correlation times for the *solute* are nearly equal to the equivalent ones of the cage, consistent with the strong coupling of solute within its cage which leads to a collective reorientation of solute and cage (e.g. $\tau_{\text{cage}}^{(2)} = 1.4$ ps, and $\tau_{\text{solute}}^{(2)} = 1.2$ ps). Solute librations within the cage are much faster ($\tau_{\text{libr}}^{(2)} = 0.12$ ps) and are comparable to the relaxation of the relative solute displacements ($\tau_r = 0.15$ ps). The solute angular momentum exhibits the fastest correlation time ($\tau^J = 0.06$ ps). While the orientational cage potential shows rapidly and slowly relaxing components ($\tau_{\omega}^f = 0.14$ ps and $\tau_{\omega}^s = 2.87$ ps, respectively), its dominant portion shows a very long persistence. © 1995 American Institute of Physics.

I. INTRODUCTION

In principle, a full description of the molecular interactions is required to explain rotational motions in liquids. In practice, however, simplified models based on Brownian motion theory are often employed to analyze such observations as spectroscopic results or transport phenomena with rather good success. In these simplified models the role of the solvent is merely a source of frictional drag, i.e. it is a continuum devoid of specific interactions with the solute. No room exists in this framework for the chemist's intuition of the liquid state as an ensemble of strongly interacting molecules.

More extensive models than are supplied by Brownian motion theory are required to analyze the effects of the molecular organization of the solvent. The picture of liquids as strongly interacting molecules without long range order suggests that a primary role should be played by the cage of solvent molecules around the solute. It can be visualized as the locally organized structure of the solvent confining the solute in a small region of the available volume because of strong interactions with nearest neighbors. As long as this confining effect has a persistent character, the forces (and the torques) exerted by the solvent cage on the solute become

highly correlated in time, in opposition to the assumption of fast fluctuating forces of Brownian motion theory. To account for these systematic forces, Brownian motion theory should be generalized by including the cage potential generated by the solvent molecules surrounding the solute in an appropriate manner.

Dielectric dispersion of polar liquids supplied the first evidence of this cage effect. In order to explain the Poley absorption in the far infrared region, N.E. Hill proposed in rather clear terms a cage picture of solute dynamics by focusing on the potential felt by the solute under the action of neighboring molecules.¹ Her key assumption was the existence of a time scale separation between fast librational motions of the solute within the cage potential, and the slow rotations of the minimum of this potential after reorganizations of the solvent. In this way the Poley absorption in the high frequency region can be explained by solute librational motions, while the Debye relaxation time measured at lower frequencies would be associated with rotation of the equilibrium orientation of the solute, viewed as a cooperative motion involving the neighbors forming the cage.

Further insights on cage effects were provided by molecular dynamics (M.D.) simulations. The first realistic calculation of an atomic liquid showed the limits of standard Brownian motion theory.² In fact, the velocity autocorrelation function displays a negative tail to be associated with the action of a confining potential. The same feature is

^{a)}On leave of absence from Department of Physical Chemistry, University of Padova.

shared by angular velocity correlation functions derived from M.D. simulations of a variety of linear molecules, like CO, N₂, O₂, Br₂, CO₂, CS₂.^{3–11} These results suggest that cage effects are intrinsic to liquids under normal conditions.

On the experimental side, manifestations of cage effects were found by different means, for example from careful analysis of infrared¹² and Raman¹³ band shapes. Also lower frequency spectroscopies like EPR can detect them when the frequency dependence of spectral densities is analyzed, showing both higher frequency and lower frequency effects.^{14,15} Even more convincing with regard to the high-frequency librational motions are spectroscopic observations in the time domain. Experimental advances which allow measurements in the subpicosecond range, have provided direct evidence of molecular librational motion within the solvent cage.^{16–18} Equivalent information can also be recovered from stimulated gain experiments of depolarized light scattering in the suitable frequency range.¹⁹

On the theoretical side, a variety of models and methods each with quite different ingredients have been proposed for the solvent cage problem. With itinerant oscillator models, the solvent cage is assimilated into a fictitious particle interacting with the solute according to a given potential. Stochastic equations are employed to describe the time evolution of such a two-particle system. Originally this method was used for the solute translational motion within the cage,²⁰ and subsequently it has been extended to rotational motion,²¹ particularly by Coffey *et al.*,²² in a planar two-particle description. Even if this procedure is very attractive for directly representing the solvent cage, it is not completely satisfactory. First of all, this is because of the artificial character of the cage representation as a particle whose mass (or momentum of inertia), as well as the momenta, are not well defined. Moreover this kind of model utilizing a fixed interaction potential cannot account for fluctuations in the strength of the cage potential. This is an important ingredient of the problem, as shown by M.D. results for the distribution of the Einstein frequencies for translational and rotational motions of test particles.¹⁰

The importance of the distribution of librational frequencies has been emphasized by Kushick who proposed a model for describing its effects on the solute rotational motion.²³ The same problem has been analyzed by Lynden-Bell and Steele by applying cumulant techniques to orientational correlation functions.²⁴ Their Gaussian cage model is based on a normal distribution of librational frequencies. Substantial agreement has been found with the correlation functions obtained from M.D. simulations, after fitting of a parameter such as the width of the librational frequency distribution. In this framework, however, a marginal role is attributed to the dynamics of the solvent cage. In particular, the fluctuations of the solute equilibrium orientation within the cage potential were not considered, whereas in the Hill picture this process is essential to rationalize the rotational dynamics at long times. In an effort to include such a process, Deb has proposed a Monte Carlo sampling of trajectories interrupted by reorganizations of the solvent cage.²⁵ Several analytical treatments of cage effects within impact theories have been

developed in relation to far-infrared and vibrational spectroscopies.^{26,27}

A completely different approach is that advocated by Stillman and Freed.²⁸ As in standard Brownian motion theory, Fokker–Planck equations are employed, but with an extended set of stochastic variables to include parameters characterizing the cage potential, and with the constraints of detailed balance rigorously applied. A formal analogy exists with itinerant oscillator models because of the overall Markovian character of both representations. But in this case no artificial particles are required, since the extra stochastic variables are directly representative of the features of the cage potential, like its strength and its stationary position, and fully three-dimensional rotations are considered. Further developments of this line of research were made by Polimeno and Freed,^{29,30} who showed the equivalence of the Stillman and Freed approach to using multi-body Fokker–Planck–Kramers equations, and obtained extensive numerical solutions to a range of cage models. These cage models include both short-time and long-time behavior of the solute, and they are related to the previous^{14,15} EPR studies. Recently, Nordio and Polimeno³¹ have applied a planar multi-body Fokker–Planck–Kramers equation to the interpretation of dielectric relaxation and far-infrared absorption signals in dipolar liquids.

The literature of theoretical models of cage effects is extensive, with contributions that elaborate the general features noted above or that develop particular aspects of the problem. In the latter context we note the treatments which include explicitly barrier crossing (jump) processes under the hypothesis that the cage potential displays a multistable structure.³² Kivelson and co-workers have related the cage effect to the differentiation of α and β relaxation processes in glasses and supercooled liquids.³³

Molecular dynamics simulations provide very detailed information about the rotational motion of liquids.^{3–11} In principle, one can use such information not only to verify the already existing theories of the solvent cage, but also for developing new and more accurate models. However, one is confronted by the problem of precisely defining the parameters characterizing the cage, so that they can be identified during a simulation. A new method has been proposed³⁴ for the translational motion of atomic liquids, that is based on a definition of the cage potential as the interaction energy between a solute and all the solvent molecules, and it must be considered as a function of solute position for fixed solvent configuration. This cage potential can easily be calculated at each instant of a M.D. run, by holding the solvent particles fixed and by computing the overall potential energy as a function of solute displacement. Because of strong confining effects on the solute due to interactions with its nearest neighbors, this potential can be approximated by its parabolic expansion. The parameters of the expansion, i.e. the location of the minimum and the curvatures, can be used as physical variables characterizing the cage potential itself. In particular, the location of the minimum is identified with the cage center, i.e. it is the stationary point for solute trajectories if the solvent is frozen. By diagonalizing the curvature matrix, one derives the principal frequencies of solute mo-

tion within the cage (to be denoted as the cage frequencies) and the corresponding principal directions which define the axes of a cage frame. All these parameters fluctuate as a result of the reorganizations of the solvent. However, because of the operational character of such a definition of "collective" cage variables, they can be exactly calculated during a M.D. simulation, thereby providing detailed statistical information about their distribution and relaxation. On the basis of this information one can develop a model which explicitly includes the cage parameters as independent stochastic variables.³⁵

A main objective of the present work is the generalization of this method to molecular liquids. Even in this case one can define the cage potential, expressed as the overall interaction energy, as a function of solute coordinates, i.e. its position and orientation, for given solvent configuration. The difficulties arise in parametrizing such a potential in order to identify the cage variables. One can perform a parabolic expansion, but because of the dependence on both translational and rotational coordinates, this leads to an increased number of parameters whose relation to relevant features of solute-solvent interactions becomes challenging.

An additional objective in this work is to examine the M.D. results to see whether a well defined collective cage potential exists and persists long enough to significantly influence the solute reorientations as proposed by Hill.¹

The parametrization of the cage variables is examined in detail in the next Section by considering an axially symmetric solute. A parabolic expansion of the cage potential is introduced under the hypothesis that the solvent hinders both translations and rotations of the molecule. In order to deal with a minimal set of cage variables, the limit of fast equilibration of solute displacement with respect to the cage center is introduced. This allows for the identification of cage variables most directly related to the rotational dynamics of the solute. In Sec. III, a M.D. simulation of liquid chlorine is analyzed in order to determine the equilibrium properties and the relaxation behavior. Section IV is dedicated to the analysis of the distribution of cage frequencies and to their separation into slow and fast components. A general overview of the M.D. results is presented in Sec. V wherein the different dynamical processes driving solute-solvent interactions and their time scales are characterized. This leads to a precise and clear statement of the role of the collective solvent cage. A summary Section concludes this paper. In the second part of the work³⁶ (hereafter called II), a stochastic model will be presented, which takes into account all the relevant features observed in the M.D. simulation.

II. THE CAGE VARIABLES

In this section, the interaction potential between the solute and the solvent is analyzed with the aim of providing a precise definition of cage variables to be calculated self-consistently during a M.D. simulation. The dependence on both the translational and rotational coordinates of the solute must be considered in order to completely represent the interaction potential.

Let us consider a rod-like solute characterized by the position \mathbf{r}^0 and the orientation $\mathbf{\Omega}^0 = (\alpha^0, \beta^0, \gamma^0)$ of the mo-

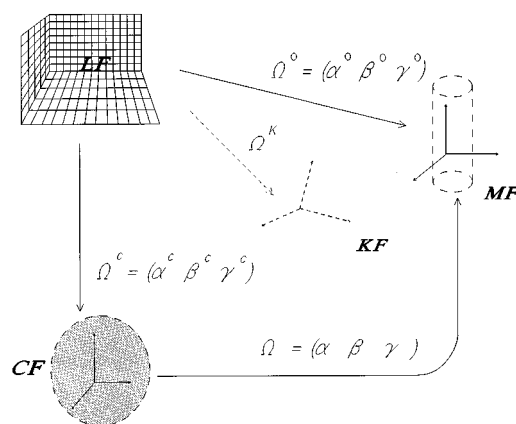


FIG. 1. Relevant frames of reference for the probe + cage system; LF laboratory frame; MF molecular frame; KF principal axis frame for the translational cage force; CF rotational cage frame.

lecular frame MF with respect to a laboratory frame LF. Figure 1 illustrates the relations among the various frames of reference employed in the derivation. The z -axis of the MF is chosen parallel to the long molecular axis. Because of the axial symmetry of the molecule, the interactions with the solvent are independent of the angle γ^0 . Therefore we leave γ^0 in the treatment since we prefer to deal with Wigner rotation matrices throughout, instead of a mixed representation that includes spherical harmonics. Also, this will more readily permit the generalization of the present treatment to non-linear molecules in the future.

For any given solvent configuration denoted concisely by Ξ (i.e. the ensemble of coordinates of solvent particles), one can calculate the interaction potential $V(\mathbf{r}^0, \mathbf{\Omega}^0, \Xi)$ between solute and solvent by adding the pair-wise contributions. The cage potential is defined as $V(\mathbf{r}^0, \mathbf{\Omega}^0, \Xi)$ to be considered for a fixed solvent configuration Ξ . The same general methodology introduced in Ref. 34 will be applied to the roto-translational problem. The main objective is that of representing in a simple form the dependence of the cage potential on the ensemble of solvent coordinates. This can be conveniently achieved by introducing a parabolic expansion of the cage potential with respect to the solute degrees of freedom. In this way the dependence on the solvent configuration is included in the coefficients of such an expansion, and they can be used as effective degrees of freedom representing the influence of the solvent on the solute.

The position \mathbf{r}^c and the orientation $\mathbf{\Omega}^c = (\alpha^c, \beta^c, \gamma^c)$ of the solvent cage are determined by the minimization of V with respect to the solute coordinates

$$\left(\frac{\partial V(\mathbf{r}^0, \mathbf{\Omega}^0, \Xi)}{\partial \mathbf{r}^0} \right)_{\mathbf{r}^0 = \mathbf{r}^c, \mathbf{\Omega}^0 = \mathbf{\Omega}^c} = 0, \quad (1)$$

$$\left(\frac{\partial V(\mathbf{r}^0, \mathbf{\Omega}^0, \Xi)}{\partial \mathbf{\Omega}^0} \right)_{\mathbf{r}^0 = \mathbf{r}^c, \mathbf{\Omega}^0 = \mathbf{\Omega}^c} = 0. \quad (2)$$

The cage coordinates necessarily depend on the solvent configuration Ξ . Since V is independent of γ^0 , condition (2)

does not determine the third angle γ^c of $\mathbf{\Omega}^c$. We assume for the moment that γ^c has been chosen according to some precise rule to be specified further on.

The set of coordinates $(\mathbf{r}^c, \mathbf{\Omega}^c)$ defines a cage frame CF, and one can then specify the solute configuration by means of relative coordinates $(\mathbf{r}, \mathbf{\Omega})$ for the displacement and the rotation of the solute from the CF to the MF. Then the cage potential can be described in terms of this new set of variables as $V(\mathbf{r}, \mathbf{\Omega}, \mathbf{\Xi})$, where the dependence on \mathbf{r}^c and $\mathbf{\Omega}^c$ is included through $\mathbf{\Xi}$. In the following we shall analyze in detail the dependence of the cage potential on the relative coordinates of the solute by leaving implicit the dependence of V on the solvent configuration $\mathbf{\Xi}$.

Some hypothesis about the solute-solvent interactions is required as a guideline in the parametrization of the cage potential. We assume that there is a strong confining effect due to the solvent such that the cage potential is characterized by a steep dependence on the solute displacement and rotation. Given these conditions, a parabolic expansion of the cage potential with respect to \mathbf{r} and to β should describe its dominant part. Note that the condition of small displacements from the equilibrium orientation does not limit the range of the angle α of $\mathbf{\Omega}$.

Thus we separate the cage potential into two parts

$$V(\mathbf{r}, \mathbf{\Omega}) = V_h(\mathbf{r}, \mathbf{\Omega}) + V_a(\mathbf{r}, \mathbf{\Omega}), \quad (3)$$

where the harmonic contribution V_h includes all the terms up to the second order in powers of \mathbf{r} and β , and V_a denotes the remaining anharmonic contributions. We assume that V_a can be neglected in the equilibrium distribution of the problem, and the following analysis is devoted to the parametrization of V_h alone. It should be mentioned, however, that the dynamical effects of the anharmonic terms are partially accounted for by the stochastic cage model (cf. paper II) through the fast fluctuating forces responsible for the frictional dissipation.

Let us first discuss the dependence of V_h on the solute orientation $\mathbf{\Omega}$. Because of the axial symmetry of the solute, V_h can be expanded in a series of Wigner matrices $D_{l,0}^j(\mathbf{\Omega})$, where, in this expansion, only the terms bearing a contribution up to second order in β need be included. Therefore components with $|l| > 2$ are excluded because

$$D_{l,0}^j \propto \exp(-il\alpha)\beta^{|l|} \quad \text{for } \beta \rightarrow 0. \quad (4)$$

The dependence on the angle α is then confined to just a few periodic functions.

By performing the expansion with respect to the solute displacement, one obtains

$$V_h(\mathbf{r}, \mathbf{\Omega}) = V^{(0)}(\mathbf{\Omega}) + \mathbf{r}^T \mathbf{V}^{(1)}(\mathbf{\Omega}) + \mathbf{r}^T \mathbf{V}^{(2)}(\mathbf{\Omega}) \mathbf{r} / 2, \quad (5)$$

$$V^{(0)}(\mathbf{\Omega}) = V_h(\mathbf{0}, \mathbf{\Omega}), \quad (6)$$

$$V_i^{(1)}(\mathbf{\Omega}) = \left(\frac{\partial V_h(\mathbf{r}, \mathbf{\Omega})}{\partial r_i} \right)_{\mathbf{r}=\mathbf{0}}, \quad (7)$$

$$V_{i,j}^{(2)}(\mathbf{\Omega}) = \left(\frac{\partial^2 V_h(\mathbf{r}, \mathbf{\Omega})}{\partial r_i \partial r_j} \right)_{\mathbf{r}=\mathbf{0}}, \quad (8)$$

where the superscript T denotes the transposed array (or matrix). Since we retain terms up to second order overall in \mathbf{r} and β , the matrix $\mathbf{V}^{(2)}(\mathbf{\Omega})$ should be evaluated at $\beta=0$, without any dependence on α . Then we can write the second order term in Eq. (5) as $\mathbf{r}^T \mathbf{K} \mathbf{r} / 2$, where $\mathbf{K} = \mathbf{V}^{(2)}(\mathbf{0})$ is the curvature matrix for the translational motion. We use for \mathbf{K} the same parametrization introduced in Ref. 34, by considering the eigenvalue problem

$$\mathbf{K} \mathbf{u}_m = k_m \mathbf{u}_m \quad (9)$$

with the principal directions \mathbf{u}_j defining the axes of the K frame (KF). The Euler angles $\mathbf{\Omega}_K$ will denote the rotation from the LF to the KF.

Let us now analyze the first order term in Eq. (5). Since the relative coordinates of the solute vanish at the minimum of V_h , it must obey the condition

$$\mathbf{V}^{(1)}(\mathbf{0}) = \mathbf{0}. \quad (10)$$

This term can also be expanded in a basis of Wigner functions, more precisely in terms of functions $D_{l,0}^j(\mathbf{\Omega})$ with $l \neq 0$ because $D_{0,0}^j(\mathbf{0}) \neq 0$ would violate Eq. (10). But if V_h includes only terms up to second order in the translational and rotational displacements, this expansion is confined to functions $D_{\pm 1,0}^j(\mathbf{\Omega})$ in agreement with Eq. (4). Moreover, these functions give rise to the same angular dependence, independent of the rank j , when terms linear in β are considered [cf. Eq. (4)]. In conclusion, the expansion can be limited to the lowest rank functions, and we write

$$\mathbf{u}_m^T \mathbf{V}^{(1)}(\mathbf{\Omega}) = c_{1,m} D_{1,0}^1(\mathbf{\Omega}) + c_{-1,m} D_{-1,0}^1(\mathbf{\Omega}), \quad (11)$$

where the components of the gradient of $\mathbf{V}^{(1)}$ with respect to the principal directions of the KF are to be considered for the sake of convenience (see next paragraph). Of course, V_h must be a real function and, therefore $c_{-1,m} = -c_{1,m}^*$.

Finally, the zeroth order term $V^{(0)}(\mathbf{\Omega})$, has to be parametrized. One should take into account that $V^{(0)}(\mathbf{\Omega})$ has a minimum at $\mathbf{\Omega} = \mathbf{0}$ and, therefore, it should obey the conditions

$$\left(\frac{\partial V^{(0)}(\mathbf{\Omega})}{\partial \varphi_x} \right)_{\mathbf{\Omega}=\mathbf{0}} = \left(\frac{\partial V^{(0)}(\mathbf{\Omega})}{\partial \varphi_y} \right)_{\mathbf{\Omega}=\mathbf{0}} = 0, \quad (12)$$

where φ is a rotation vector with components φ_p ($p=x,y$) in the CF. This condition is equivalent to

$$[M_{\pm} V^{(0)}(\mathbf{\Omega})]_{\mathbf{\Omega}=\mathbf{0}} = 0, \quad (13)$$

where $M = \partial / \partial \varphi$ is the corresponding rotation operator. Therefore, only Wigner functions $D_{l,0}^j(\mathbf{\Omega})$ with $l=0, \pm 2$ enter in the expansion of $V^{(0)}(\mathbf{\Omega})$ term. For small values of β and a fixed l , these functions give rise to the same angular dependence independent of the rank j , which then can be fixed. We shall employ second rank functions, so that

$$V^{(0)}(\mathbf{\Omega}) = b_0 D_{0,0}^2(\mathbf{\Omega}) + b_2 D_{2,0}^2(\mathbf{\Omega}) + b_{-2} D_{-2,0}^2(\mathbf{\Omega}) \quad (14)$$

with $b_{-l} = b_l^*$.

The overall potential is then written as

$$V_h = \sum_{l=0,\pm 2} b_l D_{l,0}^2(\boldsymbol{\Omega}) + \sum_{m=1}^3 (\mathbf{u}_m^T \mathbf{r}) \sum_{l=\pm 1} c_{l,m} D_{l,0}^1(\boldsymbol{\Omega}) + \sum_{m=1}^3 k_m (\mathbf{u}_m^T \mathbf{r})^2 / 2. \quad (15)$$

The strength of the cage potential is characterized by the set of coefficients \mathbf{b} for the purely rotational part, the coefficients \mathbf{k} for the translational part, and by the coefficients \mathbf{c} for the mixed components.

The ensemble of solute and cage variables required to specify at each instant the configuration of the system, is then

$$\mathbf{X}' = (\mathbf{r}, \boldsymbol{\Omega}, \mathbf{r}^c, \boldsymbol{\Omega}^c, \boldsymbol{\Omega}^K, \mathbf{k}, \mathbf{b}, \mathbf{c}) \quad (16)$$

and the equilibrium distribution should be considered as a function $P(\mathbf{X}')$ of all these variables. Under this approximation, the dependence of the distribution on the solvent configuration Ξ is parametrized through the set of cage variables, just as in the treatment of the purely translational problem.³⁴ Of course $P(\mathbf{X}')$ depends upon \mathbf{r}^c and $\boldsymbol{\Omega}^c$ only implicitly through $\mathbf{r}, \boldsymbol{\Omega}$ when dealing with homogeneous and isotropic solvents. The dependence on solute coordinates \mathbf{r} and $\boldsymbol{\Omega}$ is determined by the Maxwell-Boltzmann expression with respect to the solute-solvent interaction energy, i.e. V_h of Eq. (15):

$$P(\mathbf{X}') = f'(\boldsymbol{\Omega}^K, \mathbf{k}, \mathbf{b}, \mathbf{c}) \exp\{-V_h(\mathbf{X}')/k_B T\} \quad (17)$$

with f' a function related to the distribution of the cage variables. M.D. simulations can provide the needed detailed information about the dependence of $P(\mathbf{X}')$ on the cage variables $\boldsymbol{\Omega}^K, \mathbf{k}, \mathbf{b}$ and \mathbf{c} . Because of the large number of independent cage variables, their complete statistical analysis appears to be a prohibitive task. Given the limited accuracy in the statistics of a finite M.D. run, it would seem to be difficult to characterize the distribution with respect to each of these 15 real parameters and their correlations. Therefore, some further simplification for the equilibrium distribution is required.

We first derive a simpler description by neglecting completely the coupling between solute displacement \mathbf{r} and solute orientation $\boldsymbol{\Omega}$ in the cage potential V_h of Eq. (15). This is equivalent to assuming that the 6 cross-coefficients \mathbf{c} vanish. In this case the solute orientation is coupled only to the cage variables $\boldsymbol{\Omega}^c$ and \mathbf{b} , and one can define a reduced distribution $P(\mathbf{X}'')$ on this smaller set of variables

$$\mathbf{X}'' = (\boldsymbol{\Omega}, \boldsymbol{\Omega}^c, \mathbf{b}) \quad (18)$$

in the form

$$P(\mathbf{X}'') = f''(\mathbf{b}) \exp\left\{-\sum_{l=0,\pm 2} b_l D_{l,0}^2(\boldsymbol{\Omega})/k_B T\right\} \quad (19)$$

with only the distribution of parameters \mathbf{b} to be determined from M.D. simulations. This model with uncoupled solute rotations is very appealing because it permits a simple analysis of the M.D. data. On the other hand, the hypothesis of vanishing cross-correlation coefficients \mathbf{c} seems to be too re-

strictive a condition, which in general cannot be justified. The preferable alternative is to consider the solute orientation uncoupled to solute displacement from a dynamical point of view. Let us suppose that solute displacement \mathbf{r} with respect to the cage center is characterized by a very fast relaxation time τ_r . Then an effective distribution based on an average with respect to \mathbf{r} is sufficient to describe the system at times greater than τ_r . Because of the simple quadratic dependence on \mathbf{r} of the cage potential V_h , the integration over \mathbf{r} of the Maxwell-Boltzmann expression of Eq. (17) is easily performed

$$\int d\mathbf{r} \exp(-V_h/k_B T) \propto \exp\left\{-\sum_{l=0,\pm 2} d_l D_{l,0}^2(\boldsymbol{\Omega})/k_B T\right\}. \quad (20)$$

Thereby a reduced cage potential in terms of just the angular variables is obtained, with coefficients \mathbf{d} given as

$$d_0 = b_0 + \sum_m |c_{1,m}|^2 / 3k_m, \quad (21)$$

$$d_{\pm 2} = b_{\pm 2} - \sum_m c_{\pm 1,m}^2 / \sqrt{6}k_m.$$

In the presence of dynamically uncoupled solute rotations, the equilibrium distribution depends on a restricted set of variables

$$\mathbf{X} = (\boldsymbol{\Omega}, \boldsymbol{\Omega}^c, \mathbf{d}) \quad (22)$$

and it has a form similar to Eq. (19):

$$P(\mathbf{X}) = f(\mathbf{d}) \exp\left\{-\sum_{l=0,\pm 2} d_l D_{l,0}^2(\boldsymbol{\Omega})/k_B T\right\}. \quad (23)$$

Thus, only the distribution of coefficients \mathbf{d} , i.e. $f(\mathbf{d})$ needs to be determined from M.D. simulation.

It is our belief that this model is most appropriate for the analysis of the rotational dynamics. Of course one should check the presence of a fast time scale τ_r for the solute displacement \mathbf{r} . Nevertheless, even in cases where a time scale separation is not clearly present, this model would most likely represent the best available approximation for treating the cage problem in simple terms. Of course the model includes as a particular case the limit of vanishing rotation-translation coupling $\mathbf{c} = \mathbf{0}$, where $\mathbf{d} = \mathbf{b}$.

In order to attribute a physical meaning to the coefficients \mathbf{b} and to specify the most convenient method for their calculation during a M.D. run, it is convenient to derive Eq. (23) by following an alternative route. Let us denote by \mathbf{v} a unit vector in the x - y plane of the CF, which makes an angle ψ with the y axis: $\mathbf{v} = \mathbf{v}(\psi)$. We can analyze the interaction potential with the solvent by considering displacements \mathbf{r} , and rotations θ about $\mathbf{v}(\psi)$ of the solute for a fixed ψ . As independent variables one can use $\mathbf{q} = (\theta, \mathbf{r})$, where θ is the librational displacement of the molecule, i.e. the angle between its symmetry axis and the z -axis of the CF (note that θ cannot be identified with β because the domain

for θ is between $-\pi$ and $+\pi$). Since the cage potential has a minimum at $\mathbf{q}=\mathbf{0}$, one can write the following parabolic expansion:

$$V = V_0 + \mathbf{q}^T \mathbf{A} \mathbf{q} / 2, \quad A_{i,j} = \left(\frac{\partial^2 V}{\partial q_i \partial q_j} \right)_{\mathbf{q}=\mathbf{0}} \quad (24)$$

with matrix \mathbf{A} depending on the angle ψ . Once the cage position is identified during the M.D. simulation, this matrix can be easily evaluated as function of ψ by means of a finite difference method. The equilibrium distribution with respect to solute coordinates subject to the constraint of orthogonality between \mathbf{v} and the molecular symmetry axis, is then written as

$$P \propto \exp(-\mathbf{q}^T \mathbf{A} \mathbf{q} / 2k_B T). \quad (25)$$

By performing the integration over solute displacements \mathbf{r} according to the model of dynamically uncoupled rotations, one obtains:

$$P \propto \exp\{-\theta^2 (A_{0,0} - \mathbf{A}_{0,1} \mathbf{A}_{1,1}^{-1} \mathbf{A}_{1,0}) / 2k_B T\}, \quad (26)$$

where the matrix \mathbf{A} has been partitioned as

$$\mathbf{A} = \begin{pmatrix} A_{0,0} & \mathbf{A}_{0,1} \\ \mathbf{A}_{1,0} & \mathbf{A}_{1,1} \end{pmatrix} \quad (27)$$

with $q_0 = \theta$ and $\mathbf{q}_1 = \mathbf{r}$. An alternative form of Eq. (26) is

$$P \propto \exp\{-\theta^2 I_{\perp} \omega(\psi)^2 / 2k_B T\}, \quad (28)$$

where I_{\perp} is component of the moment of inertia perpendicular to the symmetry axis of the solute, so that

$$\omega(\psi) = I_{\perp}^{-1/2} \sqrt{A_{0,0} - \mathbf{A}_{0,1} \mathbf{A}_{1,1}^{-1} \mathbf{A}_{1,0}} \quad (29)$$

can be identified with the effective librational frequency within the solvent cage for rotations about $\mathbf{v}(\psi)$. These librational frequencies are real and positive quantities since the argument of the square root is positive for the following reasons. First, by using the partition theorem of matrices, one can show that

$$(A_{0,0} - \mathbf{A}_{0,1} \mathbf{A}_{1,1}^{-1} \mathbf{A}_{1,0})^{-1} = \mathbf{e}^T \mathbf{A}^{-1} \mathbf{e}, \quad (30)$$

where $\mathbf{e} = (1, 0, 0, 0)$. On the other hand \mathbf{A} , being a curvature matrix at a potential minimum, must be positive definite. The same holds for \mathbf{A}^{-1} if all the principal curvatures are finite. Then the right hand side of Eq. (30) is positive, since $\mathbf{w}^T \mathbf{A}^{-1} \mathbf{w} > 0$ for any vector \mathbf{w} different from zero. Note that $A_{0,0}$ could be negative, so that unphysical results (i.e. an unstable orientation with respect to the cage frame) would be obtained by using the distribution Eq. (19) and the true coefficients \mathbf{b} supplied by a M.D. simulation.

By comparing Eq. (28) with the previous result (23), and taking into account that $\theta = \pm\beta$, one can show that $\omega(\psi)^2$ can be approximated by a shifted sine function, i.e. $\sin 2(\psi + \psi_0)$. Therefore, two orthogonal directions \mathbf{v}_1 and \mathbf{v}_2 for $\mathbf{v}(\psi)$ can be derived from the maximum and the minimum of $\omega(\psi)$. They are the principal directions for the librational motions, and they are implicitly defined by the cage potential. We can use these directions as the x and y axes of the CF, so eliminating any indeterminacy of angle γ^c for the cage orientation $\mathbf{\Omega}^c$. Of course the assignment of the x axis to \mathbf{v}_1 or to \mathbf{v}_2 is arbitrary at the beginning of the M.D. simu-

lation. But in order to recover a continuous evolution of the cage orientation $\mathbf{\Omega}^c$ for a given solute, the initial assignment should be preserved with time according to the rule of least reorientation of the cage frame axes (just as for the axes of the KF, see Ref. 34).

The principal librational frequencies defined as the extrema of $\omega(\psi)$, are then associated with librational frequencies ω_x and ω_y for molecular rotations about the x and y axes, respectively, of the cage frame. They represent the most convenient parameters for describing the strength of the solvent cage in relation to the rotational dynamics of the solute, and they will be used as independent variables for the cage together with $\mathbf{\Omega}^c$. Equation (28) can be considered as the small- β limit of distribution Eq. (23), thereby establishing the relation between the coefficients b_l and the librational frequencies. That is, one can write an effective cage potential for solute rotation in the form

$$V_c(\mathbf{\Omega}, \omega) = -(I_{\perp}/6) \{ (\omega_x^2 + \omega_y^2) D_{0,0}^2(\mathbf{\Omega}) + \sqrt{3/2} (\omega_x^2 - \omega_y^2) [D_{2,0}^2(\mathbf{\Omega}) + D_{-2,0}^2(\mathbf{\Omega})] \}, \quad (31)$$

where $\omega = (\omega_x, \omega_y)$. Notice the similarity of this cage potential with the mean field potential for axial probes in a biaxial nematic phase.

The cage potential given by Eq. (31) has the correct symmetry for linear molecules with a center of symmetry, like N_2 or CS_2 . In fact $V_c(\mathbf{\Omega}, \omega)$ is unaffected by the transformation $(\alpha, \beta) \rightarrow (\alpha - \pi, \pi - \beta)$, and it has two equal minima at $\beta = 0$ and $\beta = \pi$. This cage potential, however, has too high a symmetry for describing linear molecules like OCS without a center of inversion and which are characterized by two non-equivalent minima. One can generalize the potential to this case, by taking into account that the $D_{0,0}^2$ function of Eq. (31) derives from the β^2 term of the expansion and, therefore, it can be substituted by linear combinations of the type

$$D_{0,0}^2 \rightarrow a D_{0,0}^2 + 3(1-a) D_{1,0}^1 \quad (32)$$

with an arbitrary coefficient a . The presence of a $D_{1,0}^1$ term eliminates the degeneracy of the minima. In particular for $a = 0$

$$V_c(\mathbf{\Omega}, \omega) = -(I_{\perp}/2) \{ (\omega_x^2 + \omega_y^2) D_{0,0}^1(\mathbf{\Omega}) + \sqrt{1/6} (\omega_x^2 - \omega_y^2) [D_{2,0}^2(\mathbf{\Omega}) + D_{-2,0}^2(\mathbf{\Omega})] \} \quad (33)$$

the potential with one minimum is representative of molecules A-B with much different size of atoms A and B, such that 180° flips of the symmetry axis are not accommodated in the given solvent cage. In the intermediate case of atoms A and B not very dissimilar, a choice of the coefficient $0 < a < 1$ in the previous equation seems to be required. But in dense fluids with strong confining effects, the interconversion of the solute between the two minima of the cage potential should be too rare an event to have significant effects on the solute dynamics. Therefore it should be legitimate to neglect the second minimum at $\beta = \pi$, and equivalent results should be recovered from Eq. (31) and Eq. (33) as long as

they are characterized by the same parabolic expansion at $\beta=0$. In the analysis of our M.D. simulation of a centrosymmetric molecule (Cl_2), the cage potential of Eq. (31) will be used.

Once the cage potential V_c has been parametrized, the equilibrium distribution Eq. (23) for the uncoupled rotational cage can be written as

$$P(\mathbf{\Omega}, \mathbf{\Omega}^c, \boldsymbol{\omega}) = \frac{\exp\{-V_c(\mathbf{\Omega}, \boldsymbol{\omega})/k_B T\}}{8\pi^2 \int d\mathbf{\Omega} \exp\{-V_c(\mathbf{\Omega}, \boldsymbol{\omega})/k_B T\}} P(\omega_x, \omega_y) \quad (34)$$

with the following normalization condition

$$\int d\mathbf{\Omega} d\mathbf{\Omega}^c d\boldsymbol{\omega} P(\mathbf{\Omega}, \mathbf{\Omega}^c, \boldsymbol{\omega}) = 1. \quad (35)$$

The function $P(\omega_x, \omega_y)$ is identified with the equilibrium distribution for the librational frequencies. It seems reasonable to assume that these parameters are statistically independent, so that a distribution of one variable only may be determined from the M.D. simulations,

$$P(\omega_x, \omega_y) = P(\omega_x)P(\omega_y). \quad (36)$$

Of course the statistical independence of the two librational frequencies should be confirmed by the M.D. simulations.

In summary, a complete analysis has been performed on the cage potential with the purpose of finding an efficient parametrization of the solute-solvent interactions. An effective distribution has been derived for the orientational degrees of freedom, which has a rather simple structure and depends on just two cage parameters identified with the principal librational frequencies of the molecule.

III. CALCULATION OF CAGE VARIABLES

We applied the procedure defined in the previous section to a M.D. simulation of 108 diatomic molecules interacting through a site-site Lennard-Jones (LJ) potential. The two equivalent sites are characterized by the LJ parameters $\epsilon = 2.46 \times 10^{-21}$ J and $\sigma = 3.332 \times 10^{-10}$ m, and their distance is $l = 2.099 \times 10^{-10}$ m. The temperature and the density have been chosen as $T = 178.3$ K and $\rho = 1.71 \times 10^3$ K g/m³. This system has been used in the past to simulate static and dynamic properties of liquid Cl_2 near the triple point.⁶ The leap-frog algorithm was employed to integrate the equations of motions, with a time step of 0.01 ps.

At the beginning of the simulation, the z -axis of the molecular frame for each test particle is chosen from the two directions determined by the molecular symmetry axis. This assignment is preserved with time in order to attribute a well defined meaning to the first rank orientational observables.

Given the solvent configuration, the cage position \mathbf{r}^c and orientation $\mathbf{\Omega}^c$ are obtained by locating the minimum of the interaction potential. The minimization of the five dimensional potential (which depends on \mathbf{r}^0 , α^0 , β^0) must be repeated for each molecule and each time step. This is the most time consuming part of the entire calculation. We have found that reasonable accuracy is obtained by using the principal axis method,³⁷ which does not involve the evaluation of the gradient of the potential. The actual solute position and orientation has been always taken as starting points of the pro-

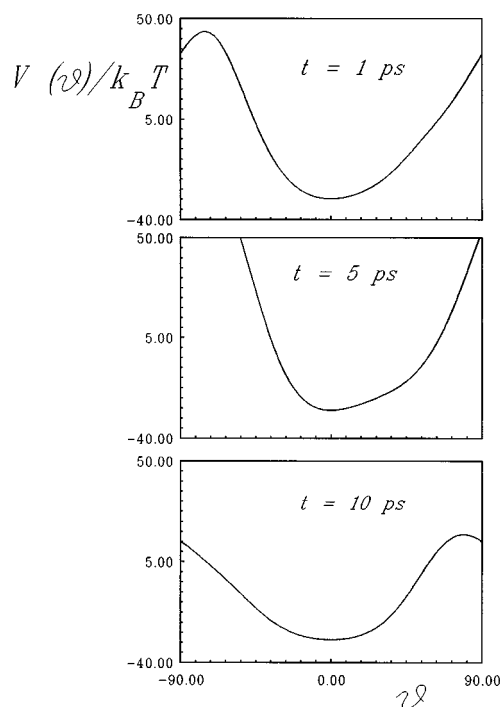


FIG. 2. Profile of the cage potential $V(\theta)$ acting on a probe molecule having translational coordinates at the minimum $\mathbf{r}^0 = \mathbf{r}^c$, and for fixed value of ψ .

cedure. Figure 2 shows the rotational potential $V(\theta)$ acting on a test molecule, obtained by keeping the position vector fixed at the translational coordinates of the minimum $\mathbf{r}^0 = \mathbf{r}^c$. Although deviations from simple parabolic shape are observed from these cage potentials, the strong confining effect of the cage boundaries is also clear. Typical *rotational* cage wells are of the order of magnitude of 50-75 $k_B T$, i.e. purely orientational relaxation of the probe within the cage, small translational adjustments are made to the trajectory and the actual energy minimum resistance path in the full roto-translational space exhibits lower energy barriers of 15-20 $k_B T$. This is the value that is compatible with the local order parameters reported in Table I for the orientation of the probe within the cage.

A sample trajectory of the translational and rotational coordinates is shown in Figures 3(a) and 3(b) respectively.

TABLE I. Equilibrium averages.

$\overline{\omega_x} = 7.44 \text{ ps}^{-1}$	$\overline{D_{00}^2(\mathbf{\Omega})} = 0.87$
$\overline{\omega_y} = 7.50 \text{ ps}^{-1}$	$\overline{D_{00}^4(\mathbf{\Omega})} = 0.66$
$\overline{\omega_x^2} = 62.00 \text{ ps}^{-2}$	
$\overline{\omega_y^2} = 62.90 \text{ ps}^{-2}$	
$\overline{\omega_x \omega_y} = 55.98 \text{ ps}^{-2}$	
$\overline{\delta \omega_i^2} = 6.62 \text{ ps}^{-2}$	
$\overline{\omega_j^2} = 3.97 \text{ ps}^{-2}$	
$\overline{\omega_s^2 - \overline{\omega_s^2}} = 2.65 \text{ ps}^{-2}$	

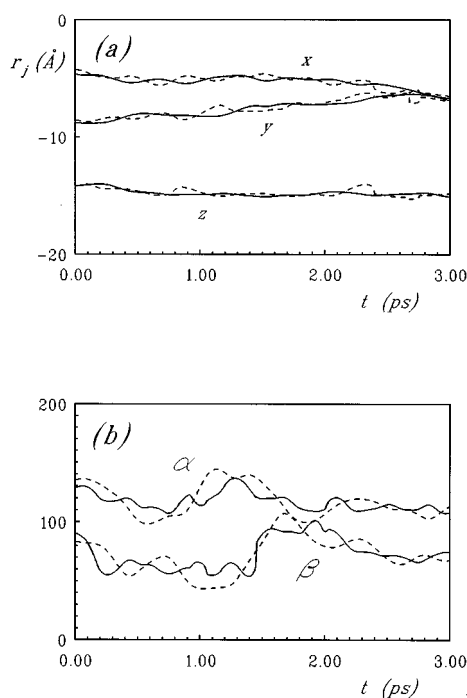


FIG. 3. (a) Time evolution of the components ($j=x,y,z$) of the test particle position r_j (continuous line) and of the cage center R_j (dashed line). (b) Time evolution of the Euler angles for the particle axis orientation α^0 , β^0 (continuous line) and of the cage center α^c , β^c (dashed line).

The jiggling motion of the translational cage coordinates, which was found in the purely translational study presented in Ref. 34, is confirmed here, together with the fact that probe and cage coordinates have the same coarse time properties, as is demonstrated by the limited range of the relative fluctuations. In the case of the rotational coordinates, however, the jiggling motion is of the probe orientational coordinates, but again the probe and cage coordinates have the same time property. It would appear that whereas the translational cage coordinates are rapidly adjusting to the solute, the rotational solute coordinates are reacting to the cage.

For the calculation of the librational frequencies, it is convenient to apply the method based on the expansion with respect to the librational angle θ , that is Eq. (29). The matrix \mathbf{A} can be easily computed by evaluating the derivatives in Eq. (24).

The assignment of x - y directions of the cage frame is made according to the maximum and the minimum value of $\omega^2(\psi)$. An example is shown in Figure 4(a). The assignment to one of these orientations is done on the basis of the principle of the least reorientation,³⁴ by taking into account the system configuration at the previous time step of the simulation. A representative trajectory of the librational frequencies is shown in Figure 4(b), while in Figure 4(c) a typical example of the time evolution of the third Euler angle γ^c specifying the cage frame is presented.

Some care is required in the initial choice of z -axis of the cage frame. At the beginning one calculates the preferred orientation of the molecular symmetry axis, and this determines two opposite directions for the z -axis of the cage frame. Within the statistical sample of all the solutes, it is

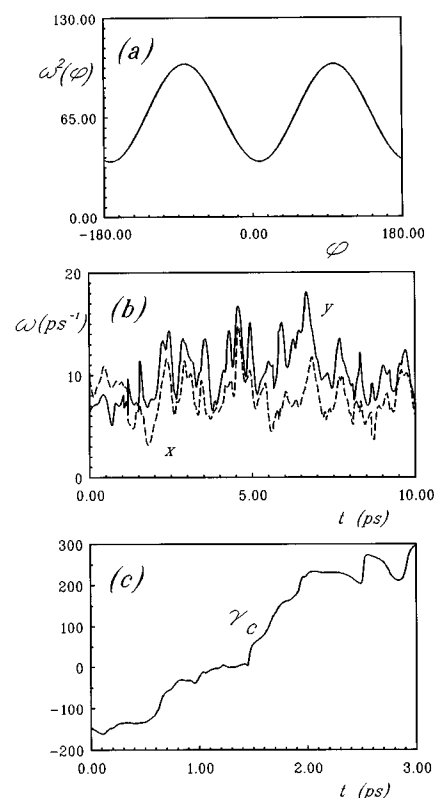


FIG. 4. (a) Profile of the function $\omega^2(\psi)$ for a test molecule. (b) Time evolution of the librational frequencies ω_x , ω_y for a test molecule. (c) Time evolution of the third Euler angle γ^c for the cage relative to a test molecule.

convenient to choose at random one of the two directions, corresponding to $\beta < \pi/2$ and $\beta > \pi/2$. This assures an even distribution with respect to angle β as in the cage potential Eq. (31). The initial assignment of the z -direction should be preserved with time according to the principle of the least reorientation.³⁴ It should be mentioned that, if one chooses an initial distribution that is unbalanced with respect to β , the correct distribution would be recovered after a sufficiently long time. But this equilibration time could be longer than the overall simulation time, if large barriers separate the two cage potential minima at $\beta=0$ and $\beta=\pi$.

The equilibrium properties of the librational frequencies have been computed, in particular averages: $\overline{\omega_i}$, $\overline{\omega_i^2}$, $\overline{\omega_x \omega_y}$. They are reported in Table I, and it is manifest that $\overline{\omega_x \omega_y} \approx \overline{\omega_x} \cdot \overline{\omega_y}$ (within statistical uncertainty), thus clearly supporting the factorization Eq. (36) of the equilibrium distribution for the librational frequencies. Under this condition, the one-dimensional distribution $P(\omega_i)$ is derived from the ensemble of M.D. data, and it is shown in Figure 5 (full line curve). In Table I we also list the averages of the Wigner functions of the relative orientation $\mathbf{\Omega}$ of the probe

$$\overline{D_{l,0}^l(\mathbf{\Omega})}. \quad (37)$$

They can be used to test the equilibrium distribution Eq. (34) with the cage potential Eq. (31) (see paper II). Only even values of l are considered, since for odd ranks the averaged values are zero.

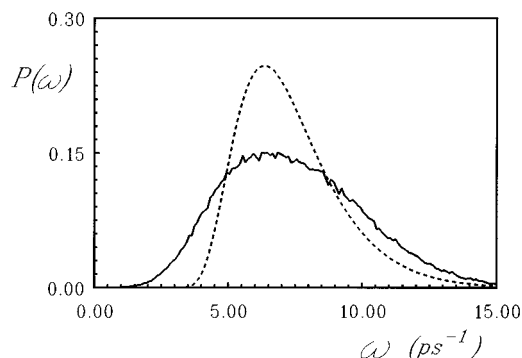


FIG. 5. Comparison between the experimental distribution $P(\omega)$ (continuous line) and the derived distribution $P_s(\omega_s)$ (dashed line) for the slow relaxing frequency ω_s .

Dynamical properties are characterized by means of the correlation functions for all the relevant variables. For the translational properties, we need just the correlation function for the relative displacement of the test particle

$$G[\mathbf{r}](t) \equiv \sum_i \overline{r_i(t)r_i(0)} \quad (38)$$

which is required to discuss the time scale separation between rotations and translations (see Sec. II) and it is presented in Fig. 6(a). The corresponding correlation time τ_r is determined from the time integral of Eq. (38).

Different kinds of orientational correlation functions can be examined, starting from the orientation $\mathbf{\Omega}^0$ of the probe with respect to the laboratory frame LF

$$G^j[\mathbf{\Omega}^0](t) \equiv \overline{D_{l,0}^j(\mathbf{\Omega}^0(t)) * D_{l,0}^j(\mathbf{\Omega}^0(0))}. \quad (39)$$

Because of the isotropy of the system, these correlation functions are independent of the index l , and the calculation is confined to ranks $j=1$ and $j=2$ (as is the case for the subsequent orientational correlation functions). They are reported in Fig. 6(b). The corresponding correlation times are denoted by $\tau^{(j)0}$. The dynamics of the cage frame orientation is described by the correlation functions

$$G_m^j[\mathbf{\Omega}^c](t) \equiv \overline{D_{l,m}^j(\mathbf{\Omega}^c(t)) * D_{l,m}^j(\mathbf{\Omega}^c(0))}. \quad (40)$$

Again, they do not depend on the laboratory index l . A definite dependence on the index m is expected and observed. Two independent processes determine the dynamics of the cage frame: the reorientation of the z -axis (i.e. the change of the most favorable orientation of the long molecular axis) and the rotation of the x - y axes following the change of the principal directions of the librational frequencies. A simple analogy exists with the anisotropic rotational diffusion of rod shaped molecules, and therefore, the same behavior may be expected for the correlation functions of Eq. (40). To confirm this hypothesis, one can compare correlation functions with different values of the index m in Fig. 7(a) ($j=1$) and in Fig. 7(b) ($j=2$). The corresponding correlation times are denoted by $\tau_m^{(j)c}$.

It is also interesting to evaluate rotational correlation functions for the relative angle $\mathbf{\Omega}$. The rotational-librational motion inside the potential well is expected to be fast com-

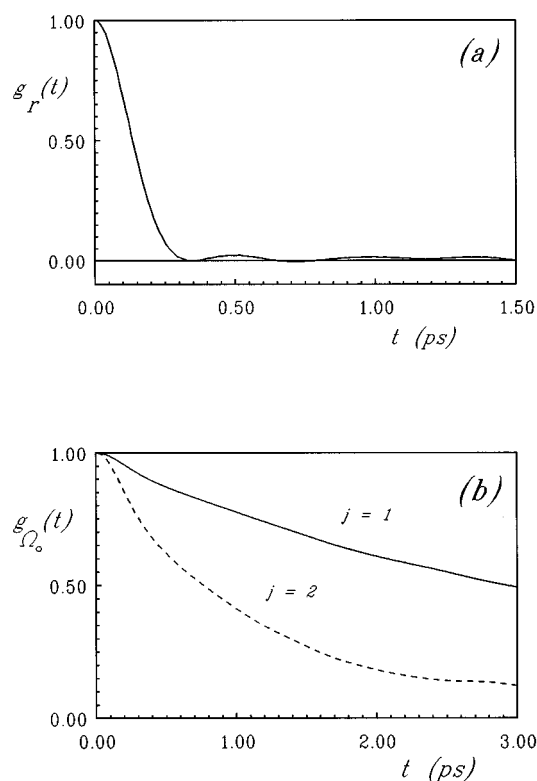


FIG. 6. (a) Normalized autocorrelation functions for the displacement between solute and cage center. (b) Normalized orientational correlation functions for the probe orientation, first rank (continuous line) and second rank (dashed line).

pared to the overall reorientation of the system molecule + cage. This is indeed observed for the second (or any even) rank correlation functions

$$G^j[\mathbf{\Omega}](t) \equiv \overline{D_{l,0}^j(\mathbf{\Omega}(t)) * D_{l,0}^j(\mathbf{\Omega}(0))}, \quad j \text{ even}. \quad (41)$$

However, first (or any odd) rank correlation functions are sensitive to the jump motion between the wells which characterize the second rank potential adopted to define the cage. Since the energy barrier is rather high, this process is extremely slow and it is not actually observable in any reasonable standard M.D. experiment. For this reason in Fig. 8 we show only the second rank correlation function for the relative orientation $\mathbf{\Omega}$. The corresponding correlation time is denoted simply as $\tau^{(2)}$. For comparison, the second rank correlation functions for the probe and the cage are also included.

Among the last correlation functions to be considered are those for the librational frequencies

$$G[\omega](t) \equiv \sum_i \overline{\delta\omega_i(t)\delta\omega_i(0)}, \quad (42)$$

where $\delta\omega_i \equiv \omega_i - \bar{\omega}_i$. This is shown in Fig. 9. One can clearly distinguish two components with rather different time scales. Therefore, two relaxation times τ_ω^f and τ_ω^s for the fast component and the slow component, respectively, are required to characterize the correlation function. Their values, reported in Table II, are obtained from a bi-exponential fit

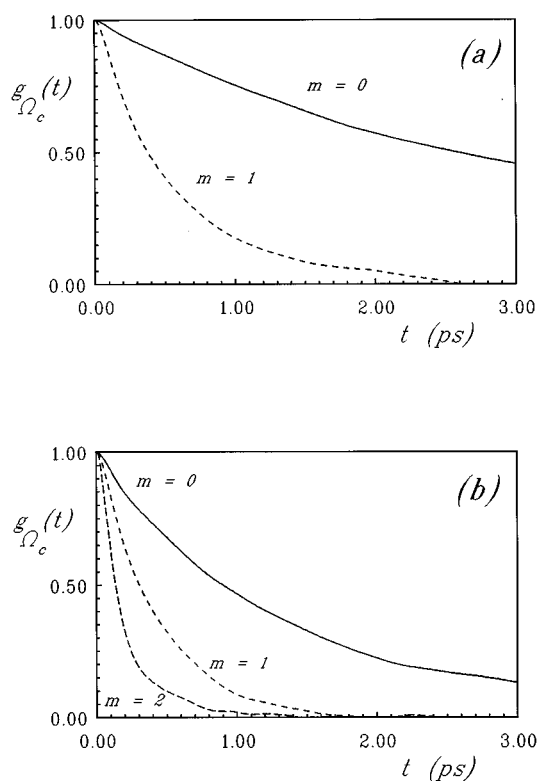


FIG. 7. (a) Normalized orientational correlation functions for the cage orientation, first rank; $m=0$ (continuous line), $m=1$ (dashed line). (b) Normalized orientational correlation functions for the cage orientation, second rank; $m=0$ (continuous line), $m=1$ (dashed line) and $m=2$ (dotted line).

ting of the data of Fig. 14. Finally, the correlation function for the angular momentum \mathbf{L} of the test particle

$$G[\mathbf{L}](t) \equiv \sum_i \overline{L_i(t)L_i(0)} \quad (43)$$

is presented in Fig. 10. In the insert we show the Fourier-Laplace transform $\tilde{g}_L(\omega)$. The corresponding correlation time is defined as τ^J . Table II collects all the calculated correlation times.

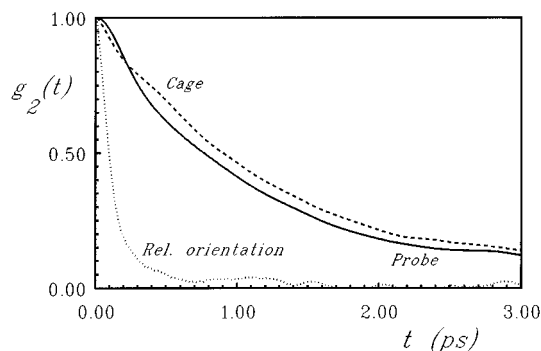


FIG. 8. Normalized orientational correlation functions for the relative orientation between molecule and cage, second rank (dotted line); for comparison the related correlation function for the probe (continuous line) and the cage (dashed line).

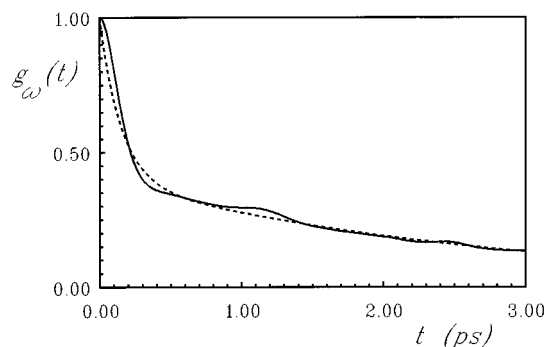


FIG. 9. Normalized correlation function for the librational frequency (continuous line) and its best bi-exponential fitting (dashed line).

IV. DISTRIBUTION OF LIBRATIONAL FREQUENCIES

It was previously observed for the case of purely translational motion in the study on liquid Ar,^{34,35} that the correlation function for the translational librational frequency $G_\omega(t)$ relaxes according to two distinct components, thereby implying that the internal reorganization of the cage structure is actually made up of a slow decay mode superimposed on a rapid local fluctuation. It appears clearly from Fig. 9 that in the present rotational system the librational frequency correlation function behaves in the same way. Correspondingly, we separate fast and slow components of the cage frequencies:³⁴

$$\omega = \omega_s + \omega_f. \quad (44)$$

This decomposition is applied to each cage frequency ω_i . The index i is left implicit because of the statistical equivalence of the two cage frequency modes. In order to determine the time scale of the two distinct modes of the cage frequencies, we suppose that they are dynamically uncoupled, and that ω_f behaves like a Gaussian stochastic variable with null average $\overline{\omega_f} = 0$, so that $\overline{\omega} = \overline{\omega_s}$. By assuming also a simple exponential decay for each component, correlation function Eq. (42) for the cage frequencies can be decomposed as:

$$G_\omega(t) = 2(\overline{\omega_s^2} - \overline{\omega_s})e^{-t/\tau_\omega^s} + 2\overline{\omega_f^2}e^{-t/\tau_\omega^f} \quad (45)$$

with τ_ω^s and τ_ω^f determining the time scales of the slow and fast components. By fitting $G_\omega(t)$ supplied by M.D. simulations according to the previous equation, one obtains both

TABLE II. Correlation times.

$\tau_r = 0.15$ ps	Relative displacement
$\tau_1^{(1)0} = 4.2$ ps	Particle reorientation ($j=1$)
$\tau_0^{(2)0} = 1.2$ ps	Particle reorientation ($j=2$)
$\tau_0^{(1)c} = 4.4$ ps	Cage reorientation ($j=1, m=0$)
$\tau_1^{(1)c} = 0.56$ ps	Cage reorientation ($j=1, m=1$)
$\tau_0^{(2)c} = 1.4$ ps	Cage reorientation ($j=2, m=0$)
$\tau_1^{(2)c} = 0.41$ ps	Cage reorientation ($j=2, m=1$)
$\tau_2^{(2)c} = 0.19$ ps	Cage reorientation ($j=2, m=2$)
$\tau^{(2)} = 0.12$ ps	Relative reorientation ($j=2$)
$\tau_\omega^f = 0.14$ ps	Fast relaxing librational frequency
$\tau_\omega^s = 2.87$ ps	Slow relaxing librational frequency
$\tau^J = 0.06$ ps	Angular momentum relaxation

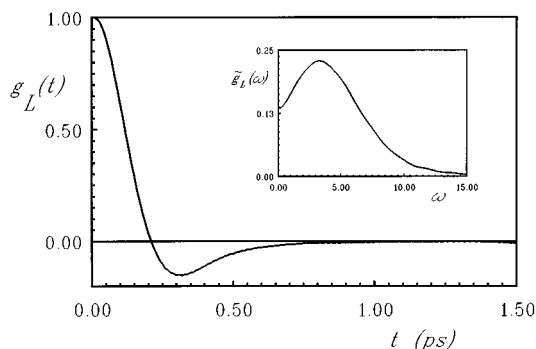


FIG. 10. Normalized autocorrelation function for the molecule angular momentum. Insert: Fourier-Laplace transform.

the pre-exponential factors (see Table I) and the relaxation times reported in Table II. The fluctuating part of the slow cage mode has the smaller weight but the longer relaxation time that is comparable to those for the overall rotation. Therefore, the fluctuations of the slow cage mode are of primary importance in the analysis of the rotational dynamics. A secondary role can be attributed to the fast cage modes, ω_f since they equilibrate in rather short times. For this reason, in the stochastic model only the slow cage components will be explicitly taken into account, and the fluctuations of ω_f will be considered as an additional contribution to the frictional dissipation of the system.

Since we only know from the M.D. experiment the probability distribution for ω , we are left with the problem of determining an effective distribution for ω_s . One can adopt a coarse graining procedure, by averaging the cage frequencies according to a suitable cutoff time τ_c which separates slow and fast cage frequencies.³⁴ Given the trajectory $\omega(t)$ for the librational frequency of a test molecule, we can define the slow component as:

$$\omega_s(t) = \frac{1}{2\tau_c} \int_{t-\tau_c}^{t+\tau_c} dt' \omega(t'). \quad (46)$$

An effective distribution $P_s(\omega_s)$ for the slow component is then obtained by the same statistical analysis used for $P(\omega)$.³⁴ Alternatively, a semi-analytical treatment can be chosen, which is described in the following paragraphs.

Let $P_t(\omega_s, \omega_f)$ be the joint probability distribution for the slow and fast cage frequencies, and $P(\omega)$ the distribution for the measured cage frequency given by Eq. (44). The relation between them is given by

$$\begin{aligned} P(\omega) &= \int d\omega_s d\omega_f \delta(\omega - \omega_s - \omega_f) P(\omega_s, \omega_f) \\ &= \int d\omega_s P(\omega_s, \omega - \omega_s) \end{aligned} \quad (47)$$

and we are interested in the distribution of the slow component only

$$P_s(\omega_s) = \int d\omega_f P_t(\omega_s, \omega_f). \quad (48)$$

Notice that $P_t(\omega_s, \omega_f)$ must be identically zero for $\omega_s + \omega_f \leq 0$ when $-\infty < \omega_f, \omega_s < +\infty$. In fact, by definition, only positive values are allowed for ω . Naturally any effective distribution found for ω_s should be practically null for $\omega_s < 0$, to be in agreement with the idea that the main contribution to the overall cage frequency resides in ω_s .

We then define a trial functional form for $P_t(\omega_s, \omega_f)$:

$$P_t(\omega_s, \omega_f) = \mathcal{H}(\omega_s + \omega_f) Q(\omega_s) g(\omega_f), \quad (49)$$

where $\mathcal{H}(\omega)$ is an unknown function which is one almost everywhere for $\omega > 0$ and is approaching zero rapidly and continuously for $\omega \rightarrow 0^+$, while it is everywhere zero for $\omega < 0$; $Q(\omega_s)$ is an unknown distribution function; finally $g(\omega_f)$ is the Gaussian distribution

$$g(\omega_f) = \frac{1}{(2\pi\overline{\omega_f^2})^{1/2}} \exp(-\omega_f^2/2\overline{\omega_f^2}) \quad (50)$$

with the width $\overline{\omega_f^2}$ previously derived. The problem is left of determining the best functional forms for $\mathcal{H}(\omega)$ and $Q(\omega_s)$. Obviously, it admits of an infinite number of solutions. However, we may consider as a first approximation that the effect of $\mathcal{H}(\omega)$ is negligible. This approximation is reasonable since it affects only the region of frequencies near zero, where $P_t(\omega_s, \omega_f)$ and $P(\omega)$ are negligible. Under this condition, we may identify $P_s(\omega_s)$ with $Q(\omega_s)$ so that

$$P(\omega) \approx \int d\omega_s P_s(\omega_s) g(\omega - \omega_s). \quad (51)$$

The solution of Eq. (51) can now be carried on in many different ways (Fourier transforms, non-linear least squares fitting etc.). We have chosen to define a functional form for $P_s(\omega_s)$ which is substituted into Eq. (51). The best fitting set of parameters characterizing the function is then determined by adopting a least square fitting criterion, with respect to the known points of $P(\omega)$. The adopted functional form for $P_s(\omega_s)$ is:

$$P_s(\omega_s) = \exp \left[- \left(\frac{\omega_s}{\omega_s^0} \right)^\mu - \left(\frac{\omega_s}{\omega_s^0} \right)^{-\nu} - \sum_{n=0}^2 a_n \left(\frac{\omega_s}{\omega_s^0} \right)^n \right] \quad (52)$$

and the following set of parameters have been calculated: $\omega_s^0 = 6.24 \text{ ps}^{-1}$, $\mu = 1.30$, $\nu = 3.59$, $a_0 = -2.20$, $a_1 = 1.19$, $a_2 = 0.406$. Figure 5 shows the comparison between $P(\omega)$ and $P_s(\omega_s)$. The new distribution is closer in shape to a simple Gaussian distribution and it assigns a negligible importance to small frequencies.

V. DISCUSSION

The results of the last two sections, especially as summarized in Tables I and II, lead to a simple but dramatic statement about the rotational dynamics of a diatomic molecule like Cl_2 . There is a very strong cage that plays a dominant role in the reorientation of a given Cl_2 molecule. In fact, the molecular reorientational correlation times $\tau^{(1)0}$ and $\tau^{(2)0}$ are very nearly the same as the equivalent correlation times $\tau^{(1)c}$ and $\tau^{(2)c}$ for the cage. This fact, plus the large cage potentials of 15-20 kT , which leads to the molecule

being very well-aligned in the cage, show that to a good first approximation the molecular reorientation is driven by the cage reorientation, i.e. the molecular reorientation is a collective process. Next we note that the cage potential reorients in a manner that strongly suggests Brownian motion. Thus, for example $\tau_0^{(1)c}/\tau_0^{(2)c} \approx 3$ (and $\tau_0^{(1)0}/\tau_0^{(2)0} \approx 3.5$), and from the cage correlation times in Table II we find that the axially symmetric Brownian diffusion expression: $D_{\perp}^c L(L+1) + (D_{\parallel}^c - D_{\perp}^c) M^2$ is roughly obeyed with $D_{\perp}^c \approx 0.12 \text{ ps}^{-1}$ and $D_{\parallel}^c \approx 1.6 \text{ ps}^{-1}$. Thus, whereas a simple experiment would show that Cl_2 undergoes Brownian reorientation, it is in reality the cage motion, to which the molecule is strongly coupled, that undergoes Brownian motion to a good approximation.

Of course, rotational librations of the molecule relative to the cage are occurring, and they are at a rate that is an order of magnitude faster than the overall reorientation. They are necessarily of low amplitude given the high orienting potential and high degree of molecular alignment within the cage (cf. Fig. 4).

This picture of a very strong cage potential, which dominates the long-time reorientation of a Cl_2 molecule, and the short time librations is precisely the model proposed earlier by Hill.

We next note that $\tau^J < \tau^{(1)0}, \tau^{(2)0}$, which is normally considered as corresponding to the regime of viscous (i.e. non-inertial) reorientational motion. For the case of simple Brownian motion, one has in this regime the Hubbard-Einstein relation, $\tau^{(2)0}/\tau^J = I/6kT$, where for Cl_2 , $I = 1.149 \times 10^{-45} \text{ kg m}^2$ yielding $\tau^{(2)0}/\tau^J = 7.71 \times 10^{-26} \text{ s}^{-2}$ at 180 K. The results of the present study yield $\tau^{(2)0}/\tau^J = 7.2 \times 10^{-26} \text{ s}^{-2}$ at 180 K. or extremely good agreement despite the fact that an individual Cl_2 molecule does not undergo simple Brownian motion. In fact, if the motion of the molecule were simple Brownian reorientation within a slowly reorienting cage potential, one expects $\tau^{(2)0}/\tau^J \gg I/6kT$.³⁸ In order that this strong inequality does not hold, it appears necessary that the frictional torques on the Cl_2 molecule be small enough so that, in the absence of the persistent strong cage potential, the motion would be in the inertial regime³⁹ for which $\tau^{(2)0} \approx \sqrt{\pi/2(I/6kT)^{1/2}} = 0.35 \text{ ps}$, which is smaller than observed. In our analysis, the persistent cage potential is taken as associated with the slowly relaxing component, whereas the rapidly relaxing component is regarded as a source of the friction. These two components represent the total harmonic potential on a Cl_2 molecule, (with a small additional anharmonic correction that we have not studied in detail), from which one readily obtains the torque acting on the molecule. From Table I we find $\overline{\omega_s^2} = 62 \text{ ps}^{-2}$ (where $\omega_s = \omega_i$, $i = x, y$) and $\overline{\omega_s^2} - \overline{\omega_s^2} = 2.65 \text{ ps}^{-2}$, so that only about 4 % of the “slow” component is fluctuating. Thus it is more accurate to refer to this as a persistent component. From the ratio $\overline{\omega_f^2}/\overline{\omega_s^2} = 0.06$ we see that the rapidly relaxing component is only a small fraction of the total harmonic potential acting on a Cl_2 molecule. This partitioning is then consistent with only a small fraction of the cage potential supplying the rapidly fluctuating torques that could provide the friction. Thus, this analysis supports the inference at the beginning of this paragraph, and we may

conclude that the dominant feature of the cage potential is its persistence rather than as a source of friction. By contrast, in a simple Brownian motion model, the total potential acting on the Brownian particle would be the rapidly fluctuating source of friction. Finally we note that τ_{ω}^f for the more rapidly fluctuating harmonic component is actually larger than τ^J (0.14 vs 0.06 ps), so that even this component does not provide the very rapidly fluctuating torques that yield a frequency-independent friction in simple Brownian motion. Its role might best be described by a frequency-dependent friction.⁴⁰ The anharmonic contributions to the potential would be expected to have similar properties to this fast component.

We next note that τ_{ω}^f and τ_r are about equal. This is consistent with the rapidly relaxing orientational component of the cage being associated with the relative translational motion of the solute within the cage. However, τ_r is significantly faster than τ_{ω}^s as well as the solute orientational relaxation times and the dominant ones for the cage ($\tau_0^{(1)c}$ and $\tau_0^{(2)c}$). Thus these processes persist over times longer than the relative translational displacements, and it appears appropriate to have assumed that they are decoupled from these displacements, in the sense that they see a time average over these displacements.

The biaxial component of the cage orientational potential does exhibit somewhat faster relaxation times (given by $\tau_1^{(1)c}$, $\tau_1^{(2)c}$, and $\tau_2^{(2)c}$), with $\tau_2^{(2)c}$ being comparable to τ_r , indicating that this feature of the cage potential may be coupled to the relative translational displacements.

Finally we can surmise from Fig. 3 that the diffusion of the position of the cage, \mathbf{r}_c is itself a slow process on the picosecond time scale consistent with the MD simulations previously described for liquid argon.³⁴ We suspect that it is this slower cage diffusion that is at least partially responsible for the fluctuations in ω_s with relaxation time τ_{ω}^s .

Although we have focussed, in this discussion (and in this paper), on the collective cage properties, one might also wish for a more *molecular* description of the cage in terms of the nearest neighbors to the solute molecule. By observing the time evolution of the ensemble of Cl_2 molecules resulting from the M.D. calculation, it is clear that there is not a very substantial local order, i.e. the neighbor molecules appear isotropically distributed in their positions with respect to a “solute” molecule, and their orientations show no close correlation with the solute. However, the nearest neighbors only diffuse away in time-scales long compared to their reorientational motion. Thus we conclude that the cage potential is indeed a collective variable that arises from summing over the interaction of many particles. In that sense there is perhaps an analogy to other collective phenomena in condensed phases, e.g. an electron that travels with its lattice distortion in a solid in the form of a polaron. This analogy is further supported by the long persistence of the dominant portion of the orientational cage potential.

VI. SUMMARY AND CONCLUSIONS

For the case of a linear diatomic molecule (Cl_2) near its triple point, it was possible to parametrize the collective cage

variables by applying some simplifying assumptions to the molecular dynamics simulations. The cage potential represents the potential acting on the solute for a fixed solvent configuration. Due to the strong confining effect of the cage, the dominant term is the harmonic contribution with respect to positional and orientational degrees of freedom of the solute relative to the cage. Consideration of the properties of these quadratic terms plus the assumption of the relative solute orientation being dynamically uncoupled from the relative solute displacement, which is justified by the faster relaxation of the latter, led to a simple form for the orientational part of the cage potential that is reminiscent of the mean field potential for axial probes in a biaxial nematic phase. It was parametrized in terms of the characteristic frequencies of libration of the diatomic molecule within the cage.

One finds from the MD simulations large and persistent orientational cage potentials with approximate parabolic shape, but significant anharmonic corrections, leading to substantial alignment, ($D_{00}^2(\Omega) = 0.87$) of the solute in the cage. The librational frequencies characterizing the orientational part of the cage potential show a dominant, mainly persistent, component with small and relatively slow fluctuations and a smaller, faster relaxing component. The orientational correlation times for the cage are consistent with an axially symmetric Brownian reorientation of the cage potential. The orientational correlation times for the solute are very nearly equal to the equivalent ones of the cage, making clear that the strong potential coupling of solute within the cage leads to a collective reorientation of solute and cage. Thus, an observation of Brownian reorientation of the solute actually implies the Brownian motion of the cage. A clear time scale separation is found between the rapidly relaxing solute angular momentum, the solute librations, the relative solute displacement, and the rapidly relaxing component of the librational frequencies on the one hand, and the much slower relaxation of the solute and cage principal axes and also the slowly fluctuating component of the librational frequencies. Intermediate between these is the relaxation of the biaxial component of the cage. These observations are utilized in paper II to construct a relatively simple stochastic model for rotational relaxation of a linear solute molecule in a solvent cage.

ACKNOWLEDGMENTS

This work was supported by National Science Foundation Grant Nos. CHE93 13167 and DMR 9210638, by the Italian Ministry for Universities and Scientific and Technological Research, and in part by the National Research Council through its Centro Studi sugli Stati Molecolari, and the Committee for Information Science and Technology. The authors thankfully acknowledge Professor P.L. Nordio for enlightening discussions. The computations reported here were performed at the Cornell Theory Center.

- ¹N. E. Hill, Proc. Phys. Soc. (London) **82**, 723 (1963).
- ²A. Rahman, Phys. Rev. A **136**, 405 (1964).
- ³B. J. Berne and G. D. Harp, Adv. Chem. Phys. **17**, 63 (1970).
- ⁴J. Barojas, D. Levesque, and B. Quentrec, Phys. Rev. A **7**, 1092 (1973).
- ⁵P. S. Y. Cheung and J. C. Powles, Mol. Phys. **30**, 921 (1975).
- ⁶E. Detyna, K. Singer, J. V. L. Singer, and A. J. Taylor, Mol. Phys. **41**, 31 (1980).
- ⁷W. A. Steele and W. B. Street, Mol. Phys. **39**, 279 (1980).
- ⁸D. J. Tildesley and P. A. Madden, Mol. Phys. **48**, 129 (1982).
- ⁹C. S. Murthy, K. Singer, and R. Vallauri, Mol. Phys. **49**, 803 (1983).
- ¹⁰C. S. Murthy and K. Singer, J. Phys. Chem. **91**, 21 (1987).
- ¹¹B. Kohler and K. A. Nelson, J. Phys. Chem. **96**, 6532 (1992).
- ¹²W. G. Rothschild, J. Soussen-Jacob, J. Bessiere, and J. Vincent-Geisse, J. Chem. Phys. **79**, 3002 (1983).
- ¹³W. G. Rothschild, R. M. Cavagnat, and P. Maraval, J. Chem. Phys. **99**, 8922 (1993); W. G. Rothschild, and R. M. Cavagnat, *ibid.* **100**, 3869 (1994).
- ¹⁴J. S. Hwang, R. P. Mason, L. P. Hwang, and J. H. Freed, J. Phys. Chem. **79**, 489 (1975).
- ¹⁵C. F. Polnaszek and J. H. Freed, J. Phys. Chem. **79**, 2283 (1975).
- ¹⁶S. Ruhman, L. R. Williams, A. G. Joly, B. Kohler, and K. A. Nelson, J. Phys. Chem. **91**, 2237 (1987); S. Ruhman and K. A. Nelson, J. Chem. Phys. **94**, 859 (1991).
- ¹⁷C. Kalpouzos, D. McMorrow, W. T. Lotshaw, and G. A. Kenney-Wallace, Chem. Phys. Lett. **150**, 138 (1988); D. McMorrow and W. T. Lotshaw, *ibid.* **178**, 69 (1991).
- ¹⁸S. R. Greenfield, A. Sengupta, J. J. Stankus, and M. D. Fayer, Chem. Phys. Lett. **193**, 49 (1992); S. R. Greenfield, A. Sengupta, J. J. Stankus, M. Terazima, and M. D. Fayer, J. Phys. Chem. **98**, 313 (1994).
- ¹⁹J. S. Friedman, M. C. Lee, and C. Y. She, Chem. Phys. Lett. **186**, 161 (1991); J. S. Friedman and C. Y. She, J. Chem. Phys. **99**, 4960 (1993).
- ²⁰F. Sears, Proc. Phys. Soc. (London) **86**, 953 (1965); P. S. Damle, A. Sjolander, and K. S. Singwi, Phys. Rev. **165**, 277 (1968).
- ²¹G. Willie, J. Phys. C.: Solid State Phys. **4**, 564 (1971).
- ²²W. T. Coffey, M. W. Evans, and G. J. Evans, Mol. Phys. **38**, 477 (1979); W. T. Coffey, P. M. Corcoran, and M. W. Evans, *ibid.* **61**, 115 (1987).
- ²³J. N. Kushick, J. Chem. Phys. **67**, 2068 (1977).
- ²⁴R. M. Lynden-Bell and W. A. Steele, J. Phys. Chem. **88**, 6514 (1984).
- ²⁵S. K. Deb, Chem. Phys. **120**, 225 (1988).
- ²⁶Yu. A. Serebrennikov, S. I. Temkin, and A. I. Burshtein, Chem. Phys. **81**, 31 (1983); A. I. Burshtein and S. I. Temkin, *Spectroscopy of Molecular Rotations in Gases and Liquids* (Cambridge University Press, Cambridge, 1994).
- ²⁷V. I. Gaiduk and Y. P. Kalmykov, J. Chem. Soc. Faraday Trans. 2 **77**, 929 (1981); V. I. Gaiduk, B. M. Tseitlin, T. A. Novskova, and J. McConnell, Physica A **197**, 75 (1993).
- ²⁸A. E. Stillman and J. H. Freed, J. Chem. Phys. **72**, 550 (1980).
- ²⁹A. Polimeno and J. H. Freed, Chem. Phys. Lett. **174**, 338, 481 (1990).
- ³⁰A. Polimeno and J. H. Freed, Adv. Chem. Phys. **83**, 89 (1993).
- ³¹P. L. Nordio and A. Polimeno, Chem. Phys. **180**, 109 (1994).
- ³²B. Lassier and C. Brot, Chem. Phys. Lett. **1**, 581 (1968); E. Praestgaard and N. G. Van Kampen, Mol. Phys. **43**, 33 (1981).
- ³³D. Kivelson and D. Mills, J. Chem. Phys. **88**, 1925 (1988); D. Kivelson and S. A. Kivelson, *ibid.* **90**, 4464 (1989).
- ³⁴G. J. Moro, P. L. Nordio, M. Noro, and A. Polimeno, J. Chem. Phys. **101**, 693 (1994).
- ³⁵A. Polimeno and G. J. Moro, J. Chem. Phys. **101**, 703 (1994).
- ³⁶A. Polimeno, G. J. Moro, and J. H. Freed (unpublished).
- ³⁷Richard P. Brent, *Algorithms for Minimization without Derivatives* (Prentice-Hall, Englewood Cliffs, NJ, 1973), Chap. VII.
- ³⁸A. Polimeno and J. H. Freed, Chem. Phys. Lett. **174**, 338 (1990).
- ³⁹W. A. Steele, J. Chem. Phys. **38**, 2411 (1962); W. B. Moniz, W. A. Steele, and J. A. Dixon, *ibid.* 2418 (1962).
- ⁴⁰L. P. Hwang and J. H. Freed, J. Chem. Phys. **63**, 118 (1975).